Available at: http://publications.ictp.it IC/2010/009

United Nations Educational, Scientific and Cultural Organization
and
International Atomic Energy Agency

THE ABDUS SALAM INTERNATIONAL CENTRE FOR THEORETICAL PHYSICS

COMPUTERIZED DETECTION OF MASSES ON MAMMOGRAMS BY ENTROPY MAXIMIZATION THRESHOLDING

Guillaume Kom[1]
LAIA, IUT-FV, University of Dschang, P.O. Box 134, Cameroon
and
The Abdus Salam International Centre for Theoretical Physics, Trieste, Italy,

Alain Tiedeu, Cyrille Feudjio
GRETMAT, LETS, ENSP, University of Yaoundé I, P.O. Box 8390, Cameroon

and

J. Ngundam
ACL, ENSP, University of Yaoundé I, P.O. Box 8390, Cameroon.

Abstract

In many cases, masses in X-ray mammograms are subtle and their detection can benefit from an automated system serving as a diagnostic aid. It is to this end that the authors propose in this paper, a new computer aided mass detection for breast cancer diagnosis. The first step focuses on wavelet filters enhancement which removes bright background due to dense breast tissues and some film artifacts while preserving features and patterns related to the masses. In the second step, enhanced image is computed by Entropy Maximization Thresholding (EMT) to obtain segmented masses. The efficiency of 98,181% is achieved by analyzing a database of 84 mammograms previously marked by radiologists and digitized at a pixel size of 343μmm × 343μ mm. The segmentation results, in terms of size of detected masses, give a relative error on mass area that is less than 8%. The performance of the proposed method has also been evaluated by means of the receiver operating-characteristics (ROC) analysis. This yielded respectively, an area (Az) of 0.9224 and 0.9295 under the ROC curve whether enhancement step is applied or not. Furthermore, we observe that the EMT yields excellent segmentation results compared to those found in literature.

MIRAMARE – TRIESTE

March 2010

[1] Regular Associate of ICTP.

I. Introduction

I.1 Necessity of computer aided diagnosis (*CAD) tools*

During 2002-2006, 95% of new cases and 97% of breast cancer deaths occurred in American women aged 40 and older [1]. The seriousness of the prognosis of breast cancer which is also the most common type of cancer to affect women in the European Union (main cause of mortality (over 12% of deaths) between 45 and 64 years old) depends mainly on how early the diagnosis is made [2]. Early detection of breast cancer is essential in reducing life fatalities [3]. When lesion is detected before cancer cells spread into the surrounding tissue, a 5-year survival rate is 97.9 % and drops sharply to 81.3% and 26.1% for regionally advanced and metastatic cancer, respectively. Mammography plays a vital role in disease diagnosis (treatment and control) and pretherapeutic management. The radiological interpretation of mammograms is a difficult task because mammographic appearance of normal tissue is highly variable. This explains why 10-30% of cancers that could have been detected are not achieved.

Manual reading is very time consuming and because of the large number of normal patients in the screening programs, radiologists need adequate technical know-how to diagnose symptoms of breast cancer especially at an early stage of development when proper treatment is adequate although they may miss some subtle symptoms. It has been shown that double reading, which includes at least two radiologists, improves the detection rate. An alternative approach is to use a computer to pre-screen the mammograms to eliminate obvious cases and provide some key information before the radiologist analyzes them. This will also reduce the manpower involved in double reading. It has been shown that the performance of radiologists can be increased by providing them with the results of CAD systems [4], [5]. Automated methods of diagnosis therefore need to be established with the aim of improving diagnostic performance by indicating suspicious areas, and a variety of computer based methods have been proposed to improve the radiologist's performance in searching for small, subtle, masked or infrequent abnormalities [4], [6]. Recently, much research has been devoted to developing reliable CAD methods [7]. A detailed report on the performance of CAD systems has been published [8]. Recent research on the analysis of digital mammograms has stimulated the development of commercial CAD systems [9]. The basic information for this detection are small grains called microcalcifications and nodules called masses (see Fig. 1) which become visible in X-ray images acquired with mammographs.

According to the type, the shape, the size and one-dimension (1D) topology of these lesions, the specialist decides to continue his investigations or not.

There are several examples in the literature of increasing lesion detection through the use of CAD methods [10], [11]. However, nowadays there are few practical CAD systems for clinical use because (a) they have not achieved sufficient performance (sensitivity and specificity); b) they have poor reproducibility and adaptivity, i.e. have a great variation in performance for different mammograms at different time and/or sites; (c) their required processing is usually not cost-effective.

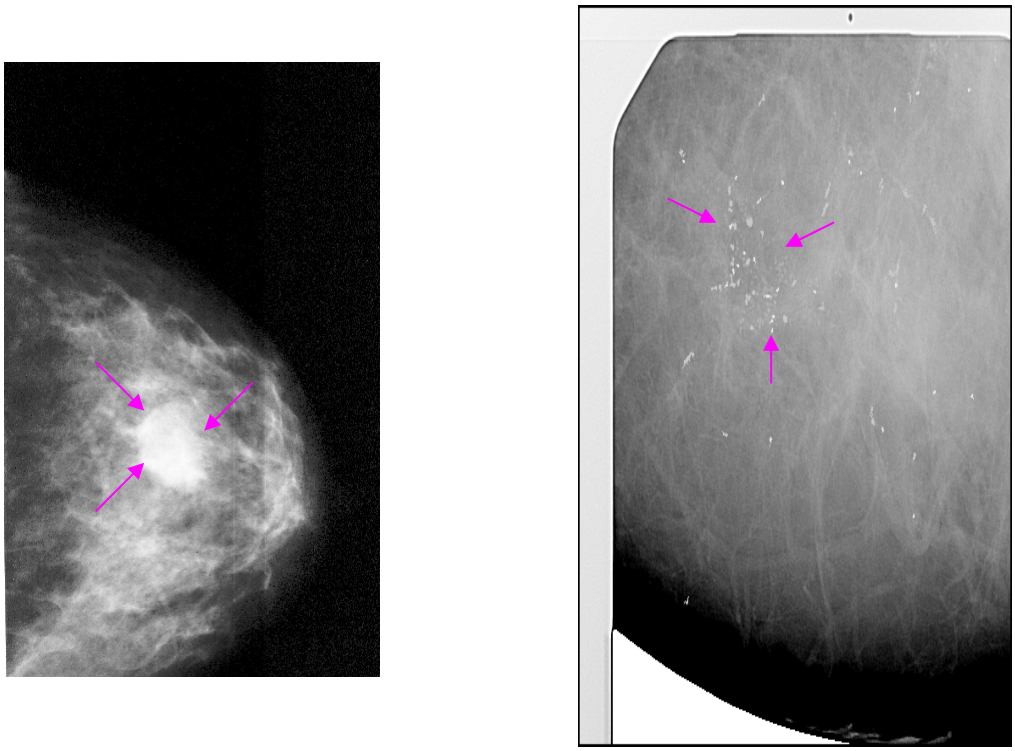

a) b)

Fig. 1: Examples of mammograms.
(a) arrows indicate mass area; (b) arrows indicate microcalcifications area.

I.2 Previous works

Many CAD methods are based on global multi-resolution analysis and local thresholding, difference image techniques, statistical approaches, neural networks, fuzzy logic, wavelet transforms and related techniques [12], [13], [14].
In [15] a uniform thresholding in a shift invariant expansion (dubbed translation invariant) built by Coifman and Donoho eliminates some unpleasant artifacts introduced by modification of the orthogonal wavelet expansion coefficients. P. Delogu et al. [16] built a CAD system for mass characterization. This is mainly on a segmentation gradient-based algorithm and on the neural classification of several features computed on the segmented mass. The value Az= 0.805±0.030 is achieved for the whole database, according to the correctly segmented masses [16]. Chan et al. [17], Davies et al. [18], and Karssemeijer [19], [20] amongst many others, have focused on microcalcifications. Kimme et al. [21], Giger et al. [22] and Miller et al. [23] have addressed asymmetry studies.
Not so many works have been done or published in the identification of regular masses and stellate lesions. The study of Eltonsy et al. [24] investigates the significance of wavelet-based and MPEG-7 homogeneous textural features in an attempt to improve the specificity of an in-house CAD system for the detection of masses in screening mammograms. The detection scheme presented relies on the concept of morphologic concentric layer analysis to identify suspicious locations in a mammogram. In the specific case of the detection of stellate lesions, Kegelmeyer [25], [26] uses Laws masks as a mechanism for detecting architectural distortions caused predominantly by the ductal patterns of the mammogram. Mudigonda et al. [27] propose the method for detection of masses in mammographic images that employs Gaussian smoothing and subsampling operations as preprocessing steps. The mass portions are segmented by establishing intensity links from the central portions of masses into the surrounding areas. Pohlman et al. [28] used a region growing algorithm for tumour segmentation, and morphological features extracted from the segmented masses for classification. Kom et al. [29] developed a CAD scheme for breast masses detection in

which the local contrast of each pixel is first modified by a linear transformation filter in order to enhance the original image. The localization of suspicious masses is then done using a local adaptive thresholding technique. A region growing technique was implemented in the mass segmentation and two different neural networks were adopted in the classification by Kinnard et al. [30]. A method for computer-aided detection of mammographic masses based on content-based image retrieval is proposed and a prototype CAD system is presented by Jin et al. [31].
This paper addresses the first two problems described above (in I-1°) in mass detection aiming for improving its performance and robustness by making the CAD method adaptive and more generalizable.

II. Basic information for diagnosis

Variable application of the mammograph and also the type of patient may yield different imaging contrast (that depends strongly on the "aspect" of the background texture of breast tissue). The detection algorithms must be robust to address these variations**.**
In studying mammograms, specific features are sought in routine examination as common indicators of malignancy [32] such as masses (of approximate regular spherical or stellate shape), microcalcification clusters and asymmetry between breasts. The low photographic density areas (as first candidates of masses) are detected with the help of a thresholding technique. This is because masses are assumed to be circular patterns that appear as white regions on mammograms.

III. Proposed computer-aided-detection system

The Key element is the method of pinpointing suspicious regions. This paper presents a new algorithm (that operates in two phases), based on detecting masses as indicators of lesions.
It shows the enhancement of mammograms using a biorthogonal wavelet decomposition filter. It further shows the detection of masses by entropy maximization thresholding. All these are examined in the following section.

III.1 General detection procedure scheme

Figure 2 shows the CAD module *(*KOM-TIEDEU 1(KT1*)* algorithm) for mass detection. Here the scanning of clinical screen films lead to a digitize mammogram. The digitized mammograms may differ from each other due to the differences in film resources and digitizers. The variation of imaging procedure and characteristics of digitizer are also a contributing factor. To reduce the influence of non breast signals on mass detection, the digitized mammograms are "standardized" by a series of pre-processing of breast area extraction; removal of Be-Be mark, noise suppression and image intensity normalisation.

III.2 Enhancement by wavelet filters (WFs)

Filtering is a technique that modifies or enhances an image. For example, an image can be filtered to emphasize certain features or remove other features. It is also a neighbourhood operation in which the value of any pixel in the output image is determined by applying some algorithms to the values of the pixels in the neighbourhood of corresponding input pixel. This paper uses the technique with wavelet filters.

III.2.1 Construction of wavelet filters

From a theoretical point, wavelets are used to characterize large sets of mathematical functions and are used in the study of operators linked to partial differential equations. From a practical view point, wavelets are used in several fields of numerical analysis, making certain complex calculations easier to handle or more precise.

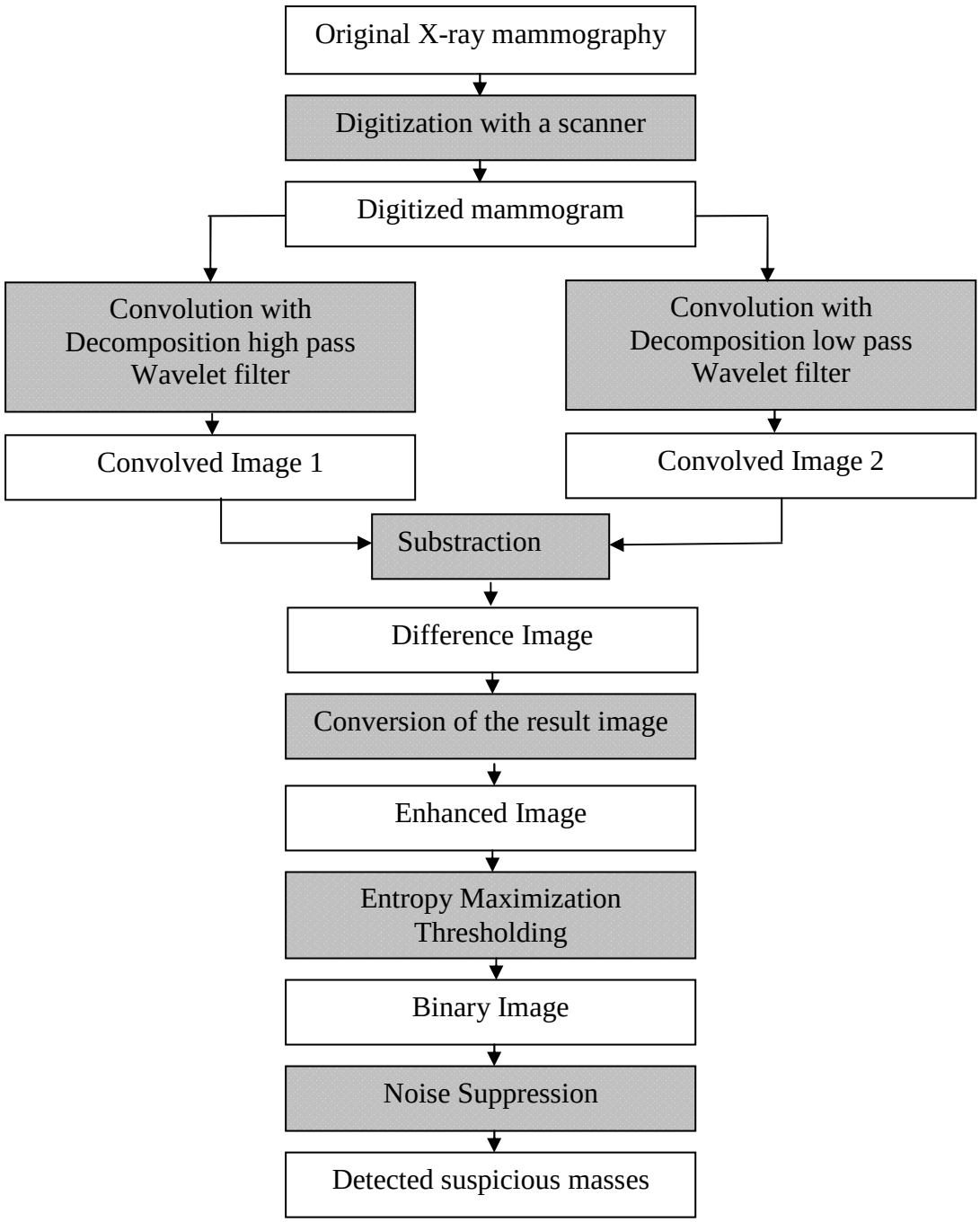

Fig. 2: The CAD module ((KT1 *algorithm) for mass detection.*

The continuous wavelet transform is a time-frequency decomposition which uses a basis of functions known as wavelets. The wavelet coefficients at the scale "s" in the transform are found by convolving the measured signal with each of the wavelets and are calculated most efficiently in the Fourier domain.

$$C(w,s) = \hat{e}(w)\varphi^*(sw) \quad (1)$$

Here *C*, $\hat{e}$ and $\hat{\varphi}$ are Fourier transforms of the wavelet coefficients C (t, s), the measured signal e (t) and the wavelet φ at the scale "s", respectively. The asterisk denotes complex conjugation. The family of wavelets $\hat{\varphi}(sw)$ are generated from a single characteristic mother wavelet $\varphi_0(w)$ over a range of scales s chosen so that $\hat{\varphi}(sw)$ span the Fourier transform of the signal and thus provide a

basis for *T(w).* The scales are often assigned to powers of 2 which is known as octave decomposition. The Fourier domain representation of time-varying filter is more complex and the reader is referred to [33] for details.

For a minimal requirement on wavelet properties, it is easy to build a new wavelet but not very interesting except if it is adapted to a specific task. For example, we can obtain wavelets adapted to a given pattern, which can then be used for accurate pattern detection. For some applications you may not be able to find a suitable wavelet among the usual ones widely available. In this case, you can design a new wavelet adapted to the problem to be solved or the task to be processed. Designing new wavelets that are well suited for the discrete wavelet transform (DWT) is more delicate and, until recently, was exclusively a topic for wavelet specialists. The lifting method proposed by Sweldens [34] facilitates this kind of construction. It allows you to generate an infinite number of discrete biorthogonal wavelets starting from an initial one. The DWT is defined by four filters as described in the fast wavelet transform (FWT) algorithm.

Two main properties of interest are:

- The perfect reconstruction property
- The link "True" wavelet (how to generate, starting from the filters, orthogonal or biorthogonal bases of the space of function of finite energy).

To illustrate the perfect reconstruction property, the following filter bank contains two decomposition filters h_a, g_a and two reconstruction filters h_s, g_s.

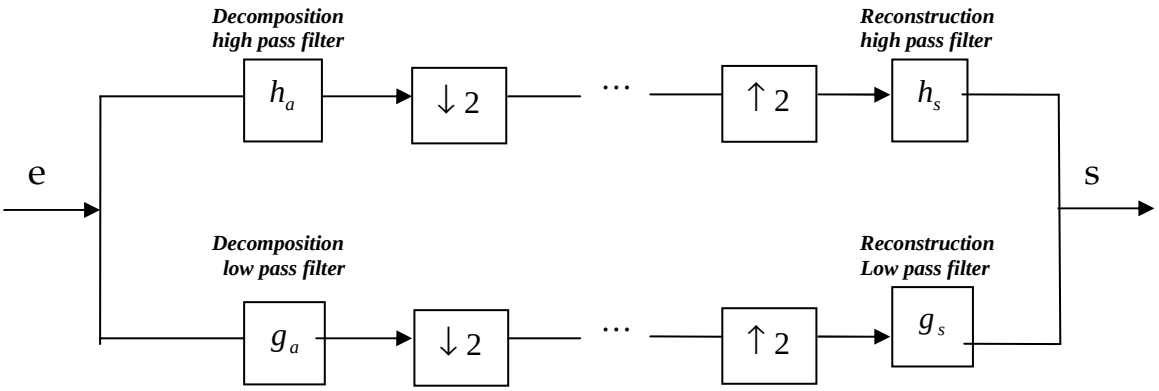

Fig. 3: Filter bank implementations of two-dimensional wavelet transform.

The symbol $(\downarrow 2)$ stands for down-sampling by 2; removing the odd-numbered samples.

The symbol $(\uparrow 2)$ stands for up-sampling by 2; inserting zeros between samples

The perfect reconstruction property can be expressed by the quality $s = e$ (up to an eventual shift or delay) where the two signals s and e are defined in Fig. 3.

For many signals, the low frequency contains the most important part. It is what gives the signal its identity. The high frequency contains, on other hand, nuances. Consider the human voice, if you remove the high frequency components, the voice sounds different, but you can still tell what's being said. However, if you remove enough of the low frequency components, you hear gibberish in the wavelet analysis. We often speak of approximation and details. The approximations are the high scale low frequency component of the signal. The details are the low scale high frequency components. Notice that the details coefficients (CD) are small and consist mainly of a high frequency noise while the approximation coefficients (CA) contain much less noise than does the original signal.

III.2.2 Implementation in mammography

The filtering process in wavelet decomposition is implemented by convolving the signal with a filter. Down-sampling and up-sampling are normally re-employed in the forward and inverse wavelet transforms, respectively. In our work, however, we maintain full resolution throughout the sub-band, decomposition for two reasons. First, from the point of view of a human observer it helps to display the sub-bands at full resolution. Second, it is easier to combine the detected pixels from each sub-band when they are at the same resolution. The implementation of a filter bank is shown in Fig. 3.
We can find in the literature [35], [36], [37] many families of wavelet (Daubechies, Coifflets, Symlets, Meyer, Biorthogonal etc…) built by specialists. We can see in table 1 below a sample of decomposition and reconstruction filter coefficients of biorthogonal wavelet basis we have used in the enhancement section.

Table 1: Sample of wavelet decomposition and reconstruction filter coefficients (Biorthogonal).

Bior1.3	h_a	0	0	-0.7071	0.7071	0	0
	g_a	-0.0884	0.0884	0.7071	0.7071	0.0884	-0.0884
	h_s	-0.0884	-0.0884	0.7071	-0.7071	0.0884	0.0884
	g_s	0	0	0.7071	0.7071	0	0
Bior2.2	h_a	0	0.3536	-0.7071	0.3536	0	0
	g_a	0	-0.1768	0.3536	1.0607	0.3536	-0.1768
	h_s	0	0.1768	0.3536	-1.0607	0.3536	0.1768
	g_s	0	0.3536	0.7071	0.3536	0	0

III.2.3 Enhancement algorithm based on convolution with wavelet filters

The algorithm is implemented by convolving a digitized mammogram with, respectively, a high pass filter and a low pass filter which constitutes a particular wavelet decomposition filter. Steps of the algorithm are described as follows:
Step 1: Load a mammogram.
Step 2: Load a particular wavelet decomposition filter which gives two vectors: one containing coefficient for a high pass filter and the other, coefficients of a low pass filter.
Step 3: Convolve the original image respectively with the low pass filter and the high pass filter loading in step 2.
Step 4: Find the difference between the two images obtained in step 3 to obtain an enhanced image.

An example can be seen on the mammogram in Fig. 4. In the original image, the enhancement filter highlights the lesion and other dense adipose tissue from the rest of the parenchymal background.

III.3 Entropy maximization thresholding

In the localization of small mass regions in digital mammograms, it is essential that the expertise and experiences of the radiologists be incorporated into computer visualisation processes for improvements in segmentation accuracy. The problem we want to solve is to detect lesions in mammogram images which appear as small bright, spot-like protrusions in the breast tissue. These lesions represent small areas in the image (8 to 9%). A method suitable for such situations is thresholding by entropy maximization.

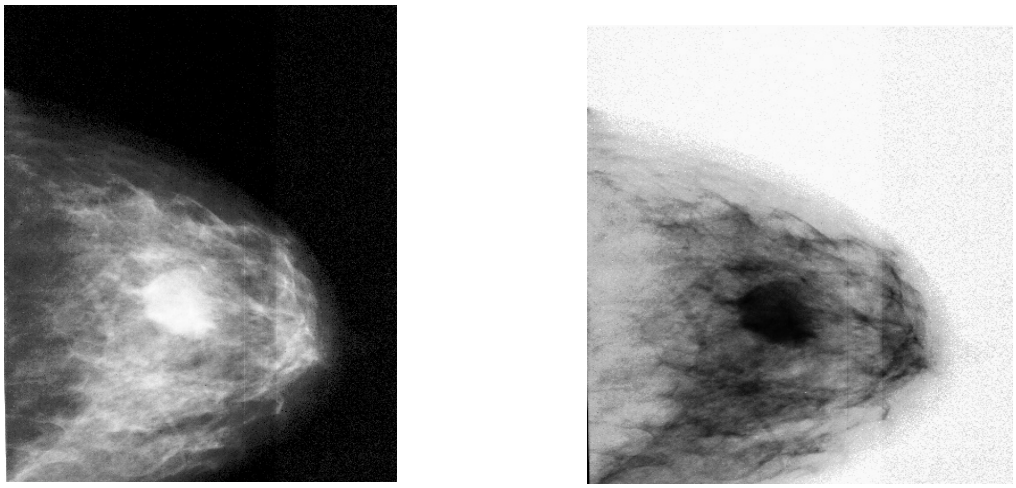

Fig. 4: An example of a mammogram on left and enhancement result on right.
NB: Images are manually rescaled for better display.

III.3.1 Basics on entropy maximization

An image is characterized by its intensity distribution, which corresponds to the observation of an object distribution through an optical system. Maximum entropy generally furnishes solutions with many artifacts [38], [39] for aperture synthesis, mainly because of the presence of point-like sources in astronomical images.
The algorithm of maximization [40] is a popular global thresholding technique. In this technique, two class problems are handled: one have typically a class with many candidates (background pixels in our case) and a class with a few candidates (mass pixels).
Let C_1 and C_2 be classes of grey level in the original mammogram. Then the entropy of the image is evaluated by the following equation:

$$H(T) = H(C_1) + H(C_2) \tag{2}$$

Here T is a variable representing pixel intensity, ranging between 0 and N. (Here, $N = 255$), $H(C_1)$ and $H(C_2)$ are the entropies of class C_1 and C_2 respectively, given by the relations:

$$H(C_1) = \sum_{i=0}^{T} \left(Pi / C_1 \right) * \ln \left(Pi / C_1 \right) \tag{3}$$

$$H(C_2) = \sum_{i=T}^{N} \left(Pi / C_2 \right) * \ln \left(Pi / C_2 \right) \tag{4}$$

Here "i" is grey level index ranging between 0 and N, Pi/C_1 and Pi/C_2 are probabilities of the grey level i in the class C_1 and class C_2, respectively.
The value of T, which gives the maximal entropy, is defined as threshold. The logarithm function in relation (3) and (4) improve classes that frequency of apparition low.

III.3.2 Entropy maximization thresholding algorithm

Step 1: We build a histogram of image to segment. This gives grey level values within the range 0 to N.
Step 2: We group the grey level of the image into 2 classes with a threshold T chosen arbitrarily among pixels of our histogram.
Step 3: We calculate the entropy $H(T)$ of the image for T varying from 0 to N.
Step 4: We identify the value of T from which $H(T)$ is maximum as the threshold "s".
Step 5: According to the condition $i > s$ pixels are grouped into two groups which lead us to a binary image with suspicious masses.

IV. Results

IV.1 Image database

Mammograms used in the following experiments are X-ray radiography images provided by the radiology unit of Yaounde Gynaeco–Obstetric and Paediatric Hospital (YGOPH) in Cameroon.
The databases consist of cranio-caudal and medio-lateral images which contained sometimes one or several masses marked by experienced radiologists. The mammograms were selected from patient's files based on visual criteria. The X-rays images were recorded with a kodak MXB film 100/NIF/30 × 40 cm screen /film combination using analogic mammography equipment "GE SENO BUCKY 8 × 2y s/DAF 66". These mammograms were digitized from a film using a high quality Acer 640 BT scanner operating at spatial resolution of 300 dpi × 300 dpi with 8 bits per pixel, with a sampling aperture of 85 μm in diameter and 12 pixels/mm sampling rate. An example of a mammogram and its detection result is shown in Fig. 5.

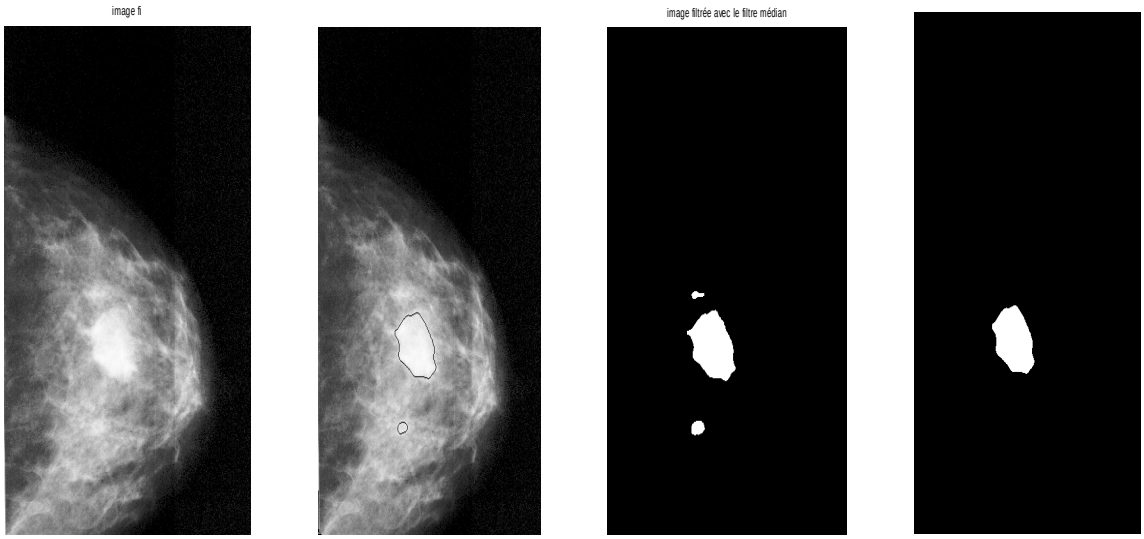

(a) (b) (c) (d)

Fig. 5: Result of segmentation procedure.
(a) Original image which includes mass; (b), (c) and (d) Result of ROIs segmented with CAD system

We carried out an evaluation of EMT algorithm (KT1) we built in terms of:
• its capacity to detect all masses,
• its capacity to maintain the size of detected masses.
We compared the size of detected masses marked by radiologists with those found by our algorithm. We carried out this comparison study in the case when enhancement step is not applied and when the enhancement step is included in the process. This led to the evaluation of the importance of the enhancement step.

IV.2 Mass detection ability

IV.2.1 In terms of number of masses detected

The data set in this study included 84 mammograms. The 84 mammograms contained 56 masses determined visually by a team of radiologists in mammography interpretation. The mammograms used in this research were divided into sets. The first set, named training database with 21 mammograms, contains 6 normal mammograms and 15 abnormal mammograms with 17 masses. This database was used to train our algorithm in order to identify the wavelets families which lead us to the best enhancement and therefore to the best threshold which gives the perfect segmentation of the mass. It is also used to select the best iteration to stop automatically our program in order to have the best segmentation. In this way, we noticed that with all orders of Daubechies wavelets, Coifflets wavelets, Discrete Meyer wavelets and Symlets wavelets, the enhancement algorithm does not change significantly an original mammogram. But the use of biorthogonal wavelets (bior1.3, bior1.5, bior3.1, bior3.3 …etc and bior2.2, bior2.4 …etc.) gives satisfactory results with the best contrast between the surrounding background and regions of interest that highlights masses. The second set named testing database, generated independently, consisting of 34 normal images and 29 abnormal images with 39 masses, was used to test the overall detection procedure. Table 2 below recapitulates figures of detection results for both sets whether enhancement step is applied or not.
An image can contain one or more masses (positives) or no mass at all (negative), and a decision for a detection result, can either be correct (true) or incorrect (false). A decision for detection result, therefore, will be one of four possible categories: true positive (TP), true negative (TN), false positive (FP), false negative (FN). FN and FP are two kinds of errors. A FN error implies that a true mass was not detected and FP error occurs when a region which is not a true mass is labelled as a mass. A TP decision is a correct judgement of an actual mass, and a TN decision means a region that does not correspond to a mass was correctly labelled. We have the following standard definitions:

$$Sensitivity: TP/(TP+FN) \quad (5)$$

$$Specificity: TN/(TN+ FP) \quad (6)$$

Table 2: Number of suspicious mass regions in each data set.

	With WFs**			**Without WFs****		
	Training Database	***Testing Database***	***Overall Database***	***Training Database***	***Testing Database***	***Overall Database***
Number of images	21	63	84	21	63	84
TP	17	37	54	17	36	53
FP	2	1	3	3	2	5
TN	3	41	44	2	41	43
FN	0	1	1	1	2	3
Diagnostic of the 2D Tool : Number of masses detected by par KT1*	19	38	57	20	38	58
Radiologists diagnostic : Number of masses marked	17	39	56	17	39	56
Sensitivity (%)	100	97,368	98,181	94,444	94,736	94,642
Specificity (%)	60	97,619	93,617	40	95,348	89,583

*: Algorithm 1 of KOM-TIEDEU **: Wavelet Filters (Enhancement step)

Sensitivity and Specificity are respectively the aptitude to detect mass and the aptitude to not detect mass when there is none effectively. They are computed according to the formulas below.
Table 2 recapitulates the detection ability of our detection approach concerning the number of detected masses TP (true positives), FP (false positives), FN (false negatives) and TN (True negatives).
The mass detection system is first evaluated with the training database. We found with this data set a sensitivity of 100%. It is then tested independently using the testing database. A good generalization performance was obtained with a sensitivity of 98,181% and specificity of 93,617%. From this table, for each database, we see the increase of sensitivity when enhancement step is applied or not (Fig. 6). This shows the influence of wavelet filters on the detection procedure. We also notice that, with the enhancement step, we obtained a fewer number of FP and FN.

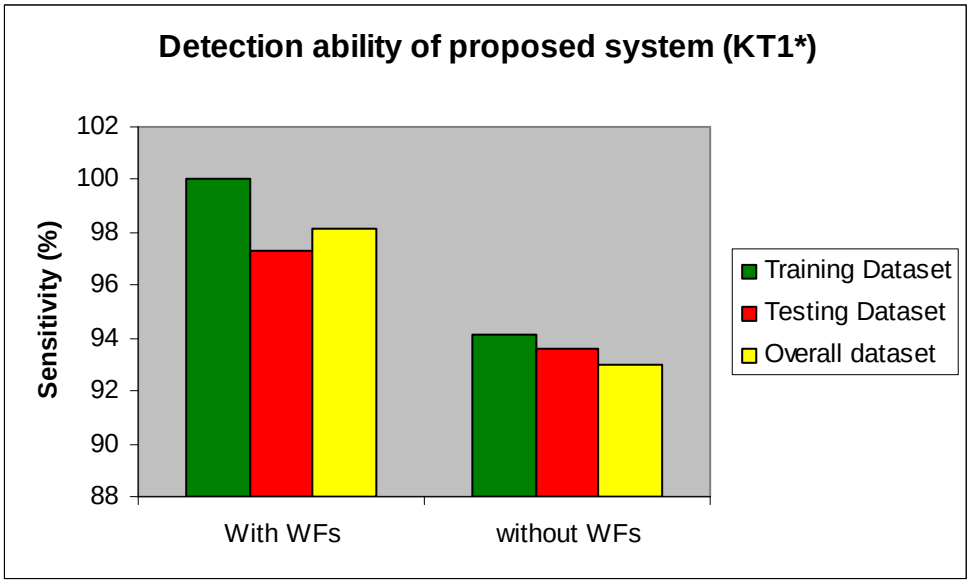

Fig. 6: Detection ability of proposed system (KT1) for each database (With and Without Wavelet Filters (WFs)).*

IV.2.2 In terms of size maintain by a mass detected

Areas of masses detected by the proposed method were compared to those marked by radiologists throughout table 3 (without WFs) and table 4 (with WFs).

Table 3: Comparison of masses' areas (Without WFs).

Mammography Pi of patient i	***N ° of Detected mass***	***Area Of Mass Marked by radiologist :S_R (in cm²)***	***Area of mass detected by par KT1* :S_A (in cm²)***	***Relative error on mass area : $\Delta S / S$ (in %)***
P1	1	8,382	7,671	8,482
	2	5,911	5,261	10,996
	3	11,777	10,483	10,987
P2	1	12,133	11,012	9,239
P3	1	5,884	5,194	11,726
	2	6,7	5,803	13,388
	3	7,333	6,296	14,141
	4	Not marked	2,563	
P4	1	11,04	9,955	9,827
P5	1	2,118	1,69	20,207
	2	6,306	5,643	10,513
	3	5,15	4,061	21,145
P6	1	2,123	1,876	11,634
	2	3,592	3,158	12,082
P7	1	3,375	2,988	11,466
	2	3,736	3,279	12,232
	3	4,472	3,634	18,738
P8	1	20,491	18,067	11,829
P9	None			
P10	None			
P11	None			
P12	None			
P13	None			

P14	1	6,766	5,321	21,356
	2	11,175	9,67	13,467
	3	10,835	9,183	15,246
P15	1	18,435	16,009	13,159
P16	1	7,14	8,2164	15,0756
P17	None			
P18	None			
P19	1	9,46	7,896	16,532
P20	1	3,72	2,98	19,892
P21	1	4,75	4,364	8,126
P22	1	5,413	4,333	19,951
P23	1	15,471	13,825	10,639
P24	1	6,355	4,934	22,360
P25	1	4,122	3,413	17,200
P26	1	12,835	10,959	14,616
P27	1	Not marked	3,311	
P28	None			
P29	1	5,924	4,546	23,261
	2	6,51	5,126	21,259
P30	1	7,276	5,962	18,059
P31	1	7,768	6,227	19,837
	2	24,977	22,233	10,986
P32	None			
P33	1	7,506	6,246	16,786
	2	6,48	5,191	19,891
P34	None			
P35	None			
P36	None			
P37	None			
P38	1	8,734	7,813	10,544
P39	None			
P40	None			
P41	1	10,135	8,717	13,991
P42	None			
P43	None			
P44	1	4,743	Not detected	
P45	1	Not marked	2,177	
P46	None			
P47	1	6,63	5,387	18,748
P48	None			

P49	None			
P50	None			
P51	1	3,876	3,212	17,131
P52	None			
P53	1	10,764	9,064	15,793
P54	1	10,287	8,866	13,813
P55	1	7,656	6,503	15,060
	2	9,738	8,431	13,421
P56	None			
P57	None			
P58	None			
P59	None			
P60	1	7,108	6,076	14,518
	2	5,825	4,574	21,476
P61	1	11,44	10,361	9,431
P62	1	22,48	20,006	11,005
P63	None			
P64	1	12,36	Not detcted	
P65	None			
P66	None			
P67	None			
P68	None			
P69	None			
P70	1	Not marked	4.236	
P71	None			
P72	None			
P73	1	15,38	13,892	9,674
	2	16,54	14,732	10,931
P74	None			
P75	None			
P76	None			
P77	1	Not marked	5,852	
P78	None			
P79	None			
P80	None			
P81	none			
P82	None			
P83	1	8,334	7,47	10,367
P84	None			

Table 4: Comparison of masses' areas (With WFs).

Mammo-Graphy Pi of patient i	***N ° of Detec-ted mass***	***Area of mass Marked by radio-logist :*** S_R ***(in cm²)***	***Area of mass Detec-ted by KT1* :*** S_A ***(in cm²)***	***Relative error on mass area :*** $\Delta S / S$ *(in %)*
P1	1	8,382	7,971	4,9034
	2	5,911	5,882	0,4906
	3	11,777	11,252	4,4578
P2	1	12,133	11,753	3,1320
P3	1	5,884	5,66	3,8069
	2	6,7	6,56	2,0896
	3	7,333	7,301	0,4364
	4	Not marked	1,958	
P4	1	11,04	10,987	0,4801
P5	1	2,118	2,2544	6,4400
	2	6,306	6,134	2,7276
	3	5,15	4,943	4,0194
P6	1	2,123	2,091	1,5073
	2	3,592	3,426	4,6214
P7	1	3,375	3,412	1,0963
	2	3,736	3,588	3,9615
	3	4,472	4,421	1,1404
P8	1	20,491	19,482	4,9241
P9	1	Not marked	2,386	
P10	None			
P11	None			
P12	None			
P13	None			
P14	1	6,766	6,423	5,0695
	2	11,175	10,964	1,8881
	3	10,835	10,33	4,6608
P15	1	18,435	18,303	0,7160
P16	1	7,14	6.891	3,4874
P17	None			
P18	None			
P19	1	9,46	9,032	4,5243
P20	1	3,72	3,701	0,5108
P21	1	4,75	4,772	0,4632
P22	1	5,413	5,406	0,1293
P23	1	15,471	15,14	2,1395
P24	1	6,355	6,081	4,3116
P25	1	4,122	3,934	4,5609
P26	1	12,835	12,056	6,0693
P27	None			
P28	None			
	1	5,924	5,529	6,6678
P29	2	6,51	6,222	4,4240
P30	1	7,276	7,161	1,5805
P31	1	7,768	7,364	5,2008
	2	24,977	23,318	6,6421
P32	None			
P33	1	7,506	7,345	2,1450
	2	6,48	6,237	3,7500
P34	None			
P35	None			
P36	None			
P37	None			
P38	1	8,734	8,808	0,8473
P39	None			
P40	None			
P41	1	10,135	9,822	3,0883
P42	None			
P43	None			
P44	1	4,743	Not detected	
P45	None			
P46	None			
P47	1	6,63	6,455	2,6395
P48	None			
P49	None			
P50	None			
P51	1	3,876	3,742	3,4572
P52	None			
P53	1	10,764	10,156	5,6485
P54	1	10,287	9,974	3,0427
P55	1	7,656	7,569	1,1364
	2	9,738	9,268	4,8265
P56	None			
P57	None			
P58	None			
P59	None			
P60	1	7,108	6,879	3,2217
	2	5,825	5,486	5,8197
P61	1	11,44	11,391	0,4283
P62	1	22,48	21,11	6,0943
P63	None			
P64	1	12,36	12,062	2,4110
P65	None			
P66	None			
P67	None			
P68	None			
P69	None			
P70	1	Not marked	3,869	
P71	None			
P72	None			

P73	1	15,38	15,092	1,8726
	2	16,54	15,897	3,8875
P74	None			
P75	None			
P76	None			
P77	None			
P78	None			

P79	None			
P80	None			
P81	None			
P82	None			
P83	1	8,334	7,844	5,8795
P84	None			

In order to compare the area of masses marked by the radiologist with those detected by our algorithm, we sketched the histograms giving the number of masses according to relative error on mass areas (see Fig. 7 and Fig. 8).

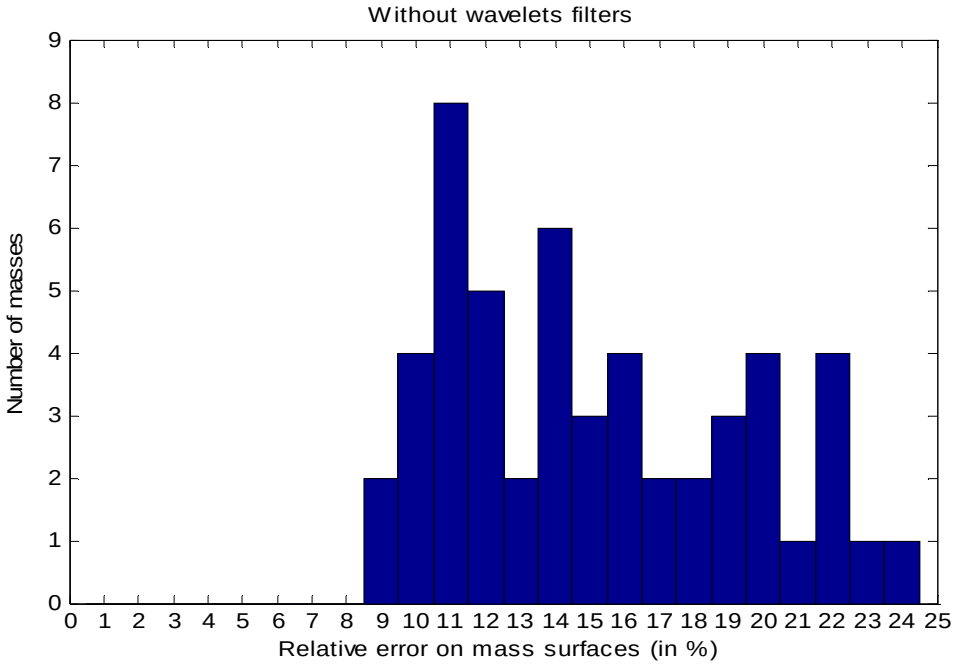

Fig. 7: Relative error on masses' surfaces (Without Wavelets Filters).

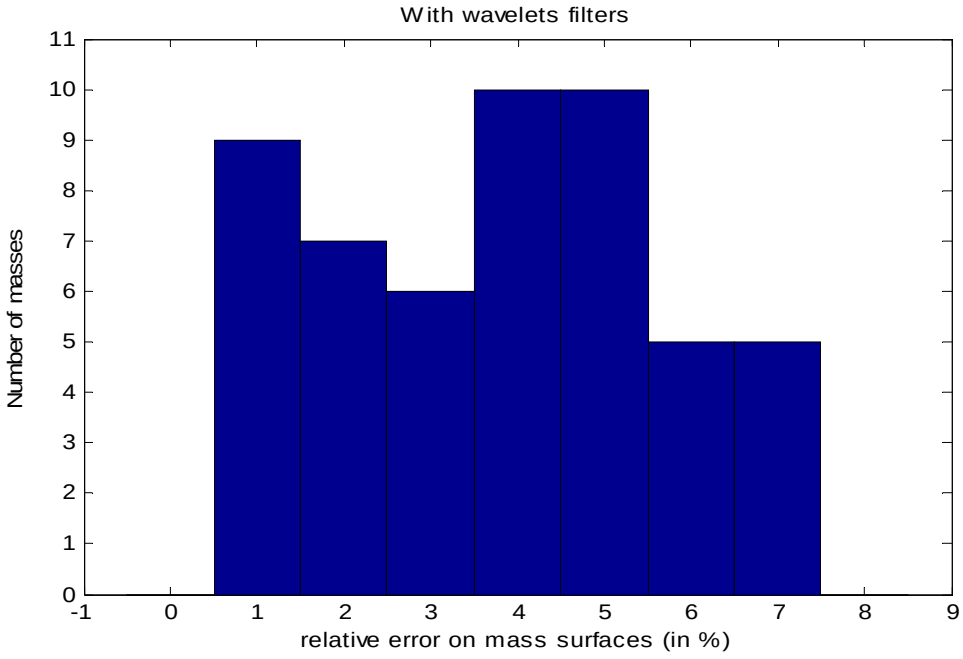

Fig. 8: Relative error on masses' surfaces (With Wavelets Filters).

On the histograms below we notice that, without enhancement step applied on EMT algorithm, relative error is always higher than 8% and reached the level of 24% (see Fig. 7). On the other hand 8% is the superior limit when wavelet filters (enhancement step) is a part of the segmentation process (see Fig. 8). Observations on Fig. 7 and Fig. 8 lead us to the conclusion that the enhancement step increases the precision in the detection of masses. The efficiency of the new algorithm we built also being pointing out according to the fact that, almost all the masses are still detected without enhancement step applied.

IV.3 System performance

IV.3.1 Computation of ROC curve

The comparison of the CAD method was made by computing the ROC (Receiver Operating Characteristic) analysis. The ROC curves were generated by varying the output threshold level. ROC analysis is based on statistical theory decision [41]. The scale of test measure can be binary, giving way to a positive and negative verdict which greatly facilitates the interpretation. But for most cases in real processes, things are not clearly defined. The distinction between positive and negative in a segmentation result is sometimes artificial because it is not always easy to confirm that a mammogram has a mass or not. When the result of this test is categorical or continuous, a break point must be found which is used as a decision threshold. The ROC curves of discrimination between mass and normal tissue regions with size feature are generated by setting different discriminating thresholds.
After bright regions were segmented on the image, the size criterion was used to determine whether the region corresponds to a mass or not. We obtained a total of 93 bright regions of interest (ROIs) that contained a range of obvious to subtle masses**.**
Knowing that a mass significant for diagnosis has a size between 3mm and 50mm [42] and taking into account that those boundaries are somehow not always certain, we divided this range into smaller intervals with attributes (1) through (5).

(1): Definitely normal	size < 2mm or size >60 mm
(2): Probably normal	50 mm < size<60 mm
(3): Uncertain	2 mm<size < 10 mm or 40 mm<size <50 mm
(4): Probably abnormal	10 mm<size < 20 mm or 35 mm<size <40 mm
(5): Definitely abnormal	20 mm < size< 35 mm

The real status for each ROI (bright region) is given by radiologists (biopsy proven) it is either a mass (class1) or not a mass (class2). Hence we found classification tables of detected ROIs according to scale (1) through (5) for each database from which we computed pairs of sensitivity (TPF: True Positive Fraction) and “1-specificity” (FPF: False Positive Fraction). From values of TPF and FPF, ROC-curves that are plotted are given in Fig. 9 and Fig. 10.

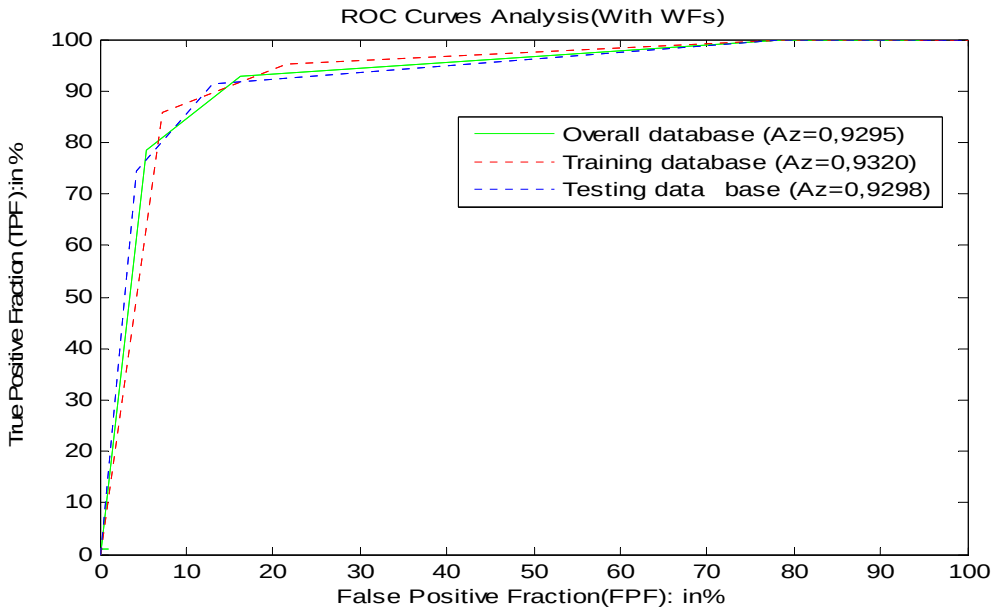

Fig. 9: Result of ROC curves analysis showing performance of databases (With Wavelets Filters).

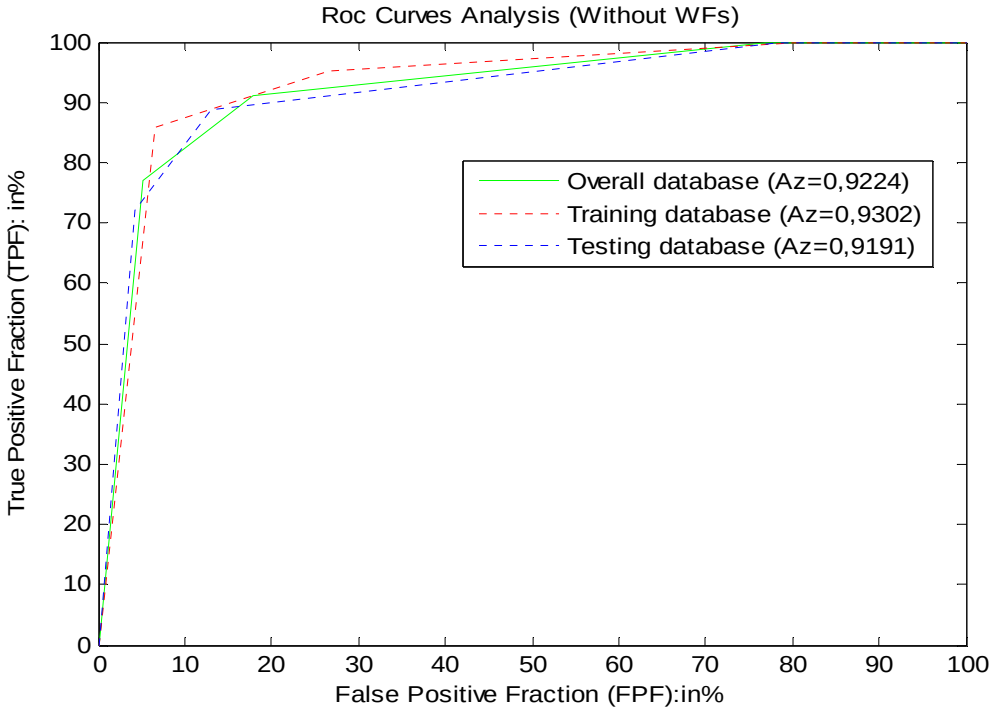

Fig. 10: Result of ROC curves analysis showing performance of databases (Without Wavelet Filters).

ROC curves (Fig. 9 and Fig. 10) show that, at the low specificity levels the two schemes (with or without enhancement) have a similar performance. No significant difference is found between the two schemes when the false positive rates are lower than 5%. At the higher specificity level levels, however, the scheme with enhancement step performs better than the one without the preprocessing.

Therefore, there is not much difference in Az value for the ROC curves with or without enhancement step. We can see in the legend section in Fig.9 and Fig.10 where their Az values increased from example, for the overall database, from 0.9224 to 0.9295 when the preprocessing step is absent or not.

IV.3.2 Complexity of our algorithm

Operations on the images shown above are costly in computing time, as they are applied to each pixel, one by one. Therefore it is obvious that the higher the resolution of the image, the higher the number of pixels, and thus more computing time will be required. However, there are differences between the application of a filter, a loop, etc. and a basic operation (arithmetic, assignation, control statements, etc.).

An algorithm is considered good, not only if it answers correctly to the problem to be solved, but also if it is faster (execution time or number of operations performed by the algorithm) and does not use too much memory (memory size or size needed to store different data structures for execution).

Hence we introduce the use of terms time complexity to evaluate what will be the fastness in computing time of an algorithm based on one or more parameters or dependent on input data and spatial complexity to evaluate the memory space that will require an algorithm according to some parameters. But today the memory is no longer a restricting parameter, although the price of RAM (Random Access Memory) has dropped dramatically in the last twenty years (furthermore, virtual memory is another answer to this problem).

Whatever the measure chosen, it is clear that the quality of the algorithm is not absolute but depends on the input data. The efficiency measures are functions of entry data. The algorithmic complexity is used to measure the performance of an algorithm.

The complexity analysis is usually done either in the best case (where the data are most favorable for the problem: number of elementary operations minimum) or in the worst case (where the data are the most ill-disposed for the problem: number of elementary operations maximum).

For our work presented above, we evaluated the execution time in the worst case because it is an upper bound of the execution time of any entry of a given size. We therefore guarantee that the algorithm will never take longer than the worst case for an instance of the same size.

After applying all the rules of customary calculation of the complexity [43], [44] we found that our main algorithm (including all sub algorithms which we have alluded to above) has a quadratic complexity O (n×m) where n and m are the dimensions (width and height) of images we used (here, 575×375). This result, compared to the characteristics of low-end computers currently available (Pentium I, II, III, IV, etc.), shows that our algorithm is efficient even though the execution time is relatively low.

IV.4 Comparison with literature and discussion

We developed a CAD system for the detection of mammographic masses with the aim of supporting radiologists in the visual diagnosis of mass. Several expert systems with a similar purpose have been recently discussed in the literature.

The mass detection algorithm built by Mudigonda et al. [27] could detect all the 13 malignant tumors in their database successfully, but achieved a success rate of only 63% in detecting the benign masses. The morphologic concentric layer detection scheme developed by Eltonsy et al. [24], achieved 93% mass detection rate with 4.8 FPs/image. The experiment results showed that the system proposed by Jin et al. [31] can achieve a ROC area index A_Z =0.84 for detection of mammographic masses. In the paper by Timp and Karssemeijer [45] the influence of the segmentation method on the performance of a CAD system was investigated, obtaining Az=0.74, 0.72 and 0.67 for segmentation based on dynamic programming, on the discrete contour model and on region growing, respectively. Christoyianni et al. [46] extensive experiments in MIAS (Mammographic Image Analysis Society) database achieved a recognition accuracy of 88.23% for the detection of all kinds of abnormalities on breast which outperforms standard textural features, widely used for cancer detection in mammograms. Sahiner et al. [47] discussed the effect of mass segmentation on

characterization: texture, morphological and spiculation features were extracted from masses segmented by a computerized technique and by the radiologist, obtaining Az =0.89 and 0.88, respectively. The performance of CAD methods for retrospective case studies, for either mass or microcalcifications cluster detection has been shown to depend on the size of image data used for testing the CAD method [48]. An advantage of our approach compared to some recent publications is that, the mass detection method proposed in this study is applicable to all types of masses (spiculated and non spiculated masses, stellar and non stellar masses, rounded masses) and independent of the size of image data. The performances it reaches are in the same range of most of the previously reported results. Compared to previously reported CAD methods, a significant improvement is made in the sensitivity of detection and reduction of the FP detection rate. The number of FP per image increased from 0.036 with enhancement step to 0.059 without enhancement step; however the number of FN per image increased to 0.012 with enhancement step to 0.036 without enhancement step. Our experimental results above showed that the system achieves a ROC area index (A_Z =0.9295 or 0.9224) for detection of mammographic masses, which is better than the best results achieved by the other known mass CAD systems. One of the major causes of missing mass detection is due to the location of masses on boundary, the extremely small size (< 2mm) and the lower contrast. The new CAD method for mass detection we developed has the following particularities:

- The segmentation of suspicious regions is adapted to accommodate different characteristics of masses and mammograms.
- The method used combined “hard” and “soft” decision making in discriminating between mass and normal tissue regions.
- Some tumours in this diagnostic database were more subtle and difficult to detect.

V. Conclusion and perspectives

We have proposed a computer system devised to support a radiologist in a small field digital mammography for breast cancer detection.
We focused on the detection of masses. The proposed algorithm operates in several phases. First the contrast of the whole mammogram is enhanced with wavelet filters. The enhancement process is based on convolution with wavelet filters. Then follows the segmentation of the enhanced image with the EMT system we built. Finally, the regions of interest detected pass through a noise suppression filter and give detected suspicious masses.
As a result, a good generalization performance was obtained with a sensitivity of 98.181% and a specificity of 93.617%. The computation of ROC curves, show that, according to the overall database, Az values increase from 0.9224 to 0.9295 whether the preprocessing step (enhan-cement by wavelets filters) is absent or not.
Compared to the radiologist point of view, their results show that the system introduces an improvement in breast cancer detection. A significant improvement in the sensitivity of detection and a reduction of FP detection rate was obtained by comparing the EMT system to previously reported CAD methods.
With the ultimate goal of discriminating benignancy from malignancy, further research work will be needed so that CAD can be an integrated and clinically useful application.

VI. Summary

A new CAD module for breast masses detection has been developed and integrated as a part of a tool to diagnose cancer on mammography. The great variability of the appearance of masses is the main obstacle for building a mass detection method. The aim of this work is to merge the knowledge and experience of radiologists in the field of reading and interpretating mammograms with the automated mass detection system we have built. Original images are first enhanced by wavelet-based filters. The resultant image is then segmented using an

entropy maximization thresholding (EMT) algorithm. As a result, over 84 mammograms on which masses had been previously marked by experienced radiologists, a good generalization performance was obtained with a sensitivity of 98.181% and a specificity of 93.617%. The computation of ROC curves show that according to the overall database, Az values increased from 0.9224 to 0.9295 when the preprocessing step (enhancement by wavelets filters) is absent or not.

A significant improvement in the sensitivity of detection and reduction of FP detection rate was obtained by comparing EMT system to previously reported CAD methods.

Compared to the radiologist point of view, their results show that the system introduces an improvement in breast cancer detection.

Acknowledgments

We would like to thank Professor J.F. Gonsu, and the employees of the Radiological Department of Yaounde Gynaeco-Obstetric and Paediatric Hospital in Cameroon who contributed to the acquisition and the reading of the mammographic database.

The authors also wish to acknowledge the Abdus Salam International Centre for Theoretical Physics (ICTP), Trieste, Italy, for financial support for Dr. Kom Guilaume Honoré during his visit. This work was partly carried out within the framework of the Associateship Scheme of ICTP.

References

[1] American Cancer Society. “Breast cancer facts & Figures 2009-2010”. Atlanta: American Cancer Society, 2009.

[2] Eurostat, “Health statistics- Atlas on mortality in the European Union”. *Office for Official Publications of the European Communities*, 2002.

[3] J.C. Fu, S.K. Lee, S.T.C. Wong, J.Y. Yeh, A.H. Wang and H.K. Wu. “Image segmentation, feature selection and pattern classification for mammographic microcalcifications”. *Computerized Medical Imaging and Graphics* vol **(**29), pp. 419–429, 2005.

[4] H.P. Chan, K. Doi, C.J. Vyborny, R.A. Schmidt, C.E. Metz, K.L. Lam, T. Ogura, Y. Wu, and H. MacMahon, “Improvement in radiologist’s detection of clustered microcalcifications on mammograms: the potential of computer aided diagnosis*”*. *Invest Radiol*. 25, 1102-1110, 1990.

[5] S. Astley, et al. “Automation in mammography: computer vision and human perception”. Int. J. *Pattern Recognition.Artif.Intell*, vol.7 (6), pp.1313-1338, 1993

[6] S.M. Astley and C.J. Taylor. “Combining for mammographic abnormalities*”*. *Proc.1st British machine Vision Conference .oxford UK*, pp.253-258, 1990.

[7] K. Doi , M.L. Giger, R.M. Nishikawa , K.R. Hoffmann, H. MacMahon, R.A. Schmidt, K.G. Chua. "Digital radiography: a useful clinical tool for computer-aided diagnosis by quantitative analysis of radiographic Images". *Acta Radiol*, vol.34, pp.426-39, 1993.

[8] “Computer-aided Detection (CAD) in Mammography”. *BCBSA technology Evaluation Center*, vol.17 (17), 2002.

[9] S. Astley, F. Gilbert, “Computer-aided detection in mammography”. *Clin.Radio*, vol.59, pp.390-399, 2004.

[10] R.L. Ellis, A.A. Meade, M.A. Mathiason, K.M. Willison, W. Logan-Young. “Evaluation of computer-aided detection systems in the detection of small invasive breast carcinoma”. *Radiology*, vol. 245(1), pp.88–94, 2007.

[11] S.J. Kim, W.K. Moon, N. Cho, J.H. Cha, S.M. Kim, J.G. Im. “Computer-aided detection in full-field digital mammography:sensitivity and reproducibility in serial examinations. *Radiology* vol.246(1), pp.71–80,2008.

[12] J.J. Heine, S.R. Deans, D.K. Cullers, R. Stauduhar, L.P. Clarke. “Multiresolution statiscal analysis of high resolution digital mammograms”. *IEEE trans Med Imaging*, vol.16, pp.503-515, 1997.

[13] T. Nestch, H.O. Peitgen, "Scale–space signatures for the detection of clustered microcalcifications in digital mammograms". *IEEE Trans Med Imaging*, vol.18, pp.774-86, 1999.

[14] W. Qian, L. Li, X. Sun, R.A. Clark. "Wavelet based image processing for digital mammography". In: Aldroubi A, laine AF, Unser MA, eds. *Wavelets Applications in signal and Image processing VIII.SPIE San Diego*, CA, pp.596-604, 2000.

[15] A.Chambolle, R.A. DeVore, N. Lee, and B. J. Lucier. "Nonlinear Wavelet image processing: Variational problems, compression, and noise removal through wavelet shrinkage". *IEEE Trans. Image processing*, vol.7, pp.319-335, 1998.

[16] D. Pasquale, E.F. Maria, K. Parnian, R. Alessandra. "Characterization of mammographic masses using a gradient-based segmentation algorithm and a neural classifier". *Computers in Biology and Medecine* (*CBM)*, vol.37, pp.1479-491, 2007.

[17] H.P. Chan,. K. Doi, et al. "Image feature analysis and computer-aided diagnosis in digital radiography: Automated detection of microcalcifications in mammography". *Medical Physics*, vol.14 (4), pp.538-548, 1987.

[18] D.H. Davies and D.R. Dance. "automatic computer detection of clustered calcifications in digital mammogram". *Phys.med.Biol.* vol.35, pp.1111-1118, 1990.

[19] N. Karssemeijer. "A stochastic model for automated detection of calcifications in digital mammograms". *Image and Vision Computing*. Vol.10, pp.369-375, 1992.

[20] N. Karssemeijer. "Recognition of clustered microcalcifications using a random field model". *SPIE Conference Biomedical Image Processing and biomedical visualisation* SPIE vol.1905, pp.776-786, 1993.

[21] C.O. Kimme, B.J. Loughlin and J. Sklansky. "Automatic detection of suspicious abnormalities in breast radiographs Data Structures". *Computer Graphics and Pattern Recognition Academic Press New York*, 1975.

[22] M.L. Giger, F. Yin, K. Doi, C.E. Metz, R.A. Schmidt, and C.J. Vyborny. "Investigation of methods for the computerized detection and analysis of mammographic masses". *SPIE Conference Medical imaging IV- Image processing SPIE,* vol.1233, pp.183-184, 1990.

[23] Miller and Astely. "Automated detection of breast asymmetries". *Internal Report Dept of medical Biophysics University of Manchester*, 1993

[24] Eltonsy, H. Nevine, Tourassi, D. Georgia, Elmaghraby, S. Adel. "Contribution of Haar wavelets and MPEG-7 textural features for false positive reduction in a CAD system for the detection of masses in mammograms". *Medical Imaging*: *Computer-Aided Diagnosis. Proceedings of the SPIE,* vol.6514, pp. 651404, 2007.

[25] W.P. Jr. Kegelmeyer. "Computer detection of stellate lesions in mammograms". *SPIE Conference Biomedical Image and Three-dimensional microscopy. SPIE, v*ol.1660, pp.446-454, 1992.

[26] W.P. Jr. Kelgelmeyer. "Evaluation of stellate lesions in mammograms". *SPIE Conference Biomedical Image Processing and biomedical visualisation SPIE,* vol.1905, pp.787-798, 1993.

[27] N.R. Mudigonda, R.M. Rangayyan, J.E. Leo Desautels. "Detection of breast masses in mammograms by density slicing and texture flow-field analysis**".** Medical *Imaging, IEEE Transactions*. Vol.20 (12), pp: 1215–1227, 2001.

[28] S. Pohlman, K.A. Powell, N.A. Obuchowski, W.A. Chicote, and S.G. Broniatowski, "Quantitative classification of breast tumours in digitized mammogram". *Med.Phys*, vol.23, pp.1337-1345, 1996.

[29] G. Kom, A. Tiedeu, M. Kom, "Automated detection of masses in mammograms by local adaptive thresholding". *Computers in Biology and Medicine (CBM).* vol.37, pp.37-48, 2007.

[30] L. Kinnard, S.B. Lo, P. Wang, M.T. Freedman, M. Chouikha, "Separation of malignant and benign masses using image and segmentation features". *Medical Imaging 2003: Image Processing,* vol. 5032, pp. 835–842, 2003.

[31] R. Jin, B. Meng, E. Song, X. Xu, L. Jiang. "Computer-aided detection of mammographic masses based on content-based image retrieval". *Medical Imaging*: *Computer-Aided Diagnosis. Proceedings of the SPIE,* Vol.6514, pp. 65141, 2007.

[32] Juhl. J.Paul & Juhl's. "Essentials of roentgen interpretation". *4th edition, Harper & row*. pp.340-345, 1982.

[33] G.F Margrave."Theory of nonstationary linear filtering in the Fourier domain with application to time-variant filtering". *Geophysics*, vol.63 (1), pp.244-259, 1998.

[34] W. Sweldens, J. Siam. “The lifting Scheme: A construction of second generation of wavelets”. *Math anal*, vol.29 (2), pp.511-546, 1998.
[35] I. Daubechies, Ten Lectures on wavelet. Philadelphia, PA: SIAM, 1992.
[36] M. Vetteri and C. Herley. “Wavelet and filter banks: Theory and design”. *IEEE Trans. Acoust., Speech Signal Processing*, vol.40, pp.2207-2232, 1992.
[37] W. Sweldens. “The lifting scheme: A custom-design construction of biorthogonal wavelets”. *Appl comput. Harmon Anal.*, vol.3, pp.186-200, 1996.
[38] J. Cohen “Tests of photometric accuracy of image restoration using the maximum entropy algorithm”. *Astrophys*, J.101, pp.734-737, 1991.
[39] T.J. Cornwell, “Deconvolution for real and synthetic aperture” , in *Astronomical Data Analysis software and system* I, D.M Worral, C. Biemesderfer, and J.Barnes, eds Astronomical society of the Sacific San Francisco , Calif, pp.163-169, 1992.
[40] J. N. Kapur, P.K. Sahooo, and A.K.C. Wong. “A new method for grey level picture thresholding using the entropy of histogram”. *Computer vision, Graphics and Image Processing*, vol.29, pp.273-285, 1985.
[41] J.M. Daigle. “ L’utilisation des courbes ROC dans l’évaluation des tests diagnostiques de laboratoires clinique : application à l’étude de la pneumonite d’hypersensibilité ”. *Thèse pour l’obtention du grade de maitre ès sciences (M.Sc). Département de mathématiques et de statistique. Faculté des Sciences et de Genie. Université de Laval*, Décembre 2002.
[42] L.Huai, Y.Wang, K.J.Ray Liu, B.L Shih-Chung, and M.T Freedman. “Computerized radiographic mass detection Part II: Decision Support by featured database visualisation and modular neural networks”. *IEEE.Trans.Med.Imaging*, vol.20 (4), pp. 302-313, 2001.
[43] A. Pozniak. “Entraînement de CAD’s en mammographie”. *Mémoire réalisé en vue de l’obtention du grade de Licencié en Informatique au Centre de Recherche en Modélisation Moléculaire.* Institut d’Informatique, Faculté des Sciences Université de Mons-Hainaut (UMH), Académie Universitaire de Wallonie-Bruxelles, 2007.
[44] C. Froidevaux, M.C. Gaudel, M. Soria, Types de données et algorithmiques, *Ediscience International*, 1994.
[45] S. Timp, N. Karssemeijer. “A new 2D segmentation method based on dynamic programming applied to computer aided detection in mammography”. *Med. Phys, vol.*31 (5), pp.958–971, 2004.
[46] I. Christoyianni, A. Koutras, E. Dermatas, G. Kokkinakis. “Computer aided diagnosis of breast cancer in digitized mamogramms”. *Computerized medical Imaging and Graphics*, vol.26, pp.309-319, 2002.
[47] B. Sahiner, N. Petrick, H.P. Chan, L.M. Hadjiiski, C. Paramagul, M.A. Helvie, M.N. Gurcan.”Computer-aided characterization of mammographic masses: accuracy of mass segmentation and its effects on characterization”. *IEEE Trans. Med. Imaging*, vol.20 (12) pp.1275–1284, 2001.
[48] K. Doi. “Overview of state of the art and future requirements, session 5B, Image processing and computer Assisted Diagnosis (CAD)”. *Office of common’s Health (OWH) workshop on digital mammography Washington DC*, June-1-2, 1997.